Fluorogenic thiazole orange TOTFO probes stabilise parallel DNA triplexes at pH 7 and above

Supplementary Information

DOI: 10.1039/x0xx00000x

Sarah Walsh,[a, b] Afaf Helmy El-Sagheer[a, c] and Tom Brown[a]

[a] *Department of Chemistry, University of Oxford, 12 Mansfield Road, Oxford, OX1 3TA, UK.*
Email: tom.brown@chem.ox.ac.uk
[b] *ATDBio Ltd., Robert Robinson Ave, Oxford, OX4 4GA, UK.*
[c] *Chemistry Branch, Department of Science and Mathematics, Faculty of Petroleum and Mining Engineering, Suez University, Suez 43721, Egypt*

Table of Contents

Section A. Materials and Methods

SA.1. General Synthesis

Reagents were purchased from Sigma-Aldrich, Alfa Aesar or Fisher Scientific and were used without further purification. Dry solvents were obtained using the MBraun SPS bench top solvent purification system. Thin layer Chromatography (TLC) was performed using Merck TLC silica gel 60 F254 plates (0.22 mm thickness, aluminium coated). Compounds were visualised using UV irradiation and also stained with potassium permanganate ($KMnO_4$). Column chromatography was carried out under pressure (argon) using Merck Geduran® 60Å (40-63 µm) silica gel. ^{1}H NMR spectra were measured at 400 MHz on a Bruker DPX400 (AVIIIHD 400) spectrometer. ^{13}C NMR spectra were measured at 101 MHz on a Bruker DPX400 spectrometer. Chemical shifts are given in ppm. ^{1}H and ^{13}C NMR spectra were internally referenced to the residual un-deuterated solvent signal.[1] Assignments of the compounds were aided by COSY (^{1}H - ^{1}H) and HSQC (^{1}H - ^{13}C) experiments. Spectra were reprocessed using Mestre Nova software. Low-resolution mass spectra were recorded using electrospray ionisation (ESI^+ or ESI^-) on a Waters ZMD quadrupole mass spectrometer in HPLC grade methanol or acetonitrile.

5-(1-propargylamino)-2´-deoxyuridine (pdU) and 2'-amino-ethoxythymidine phosphoramidites were synthesised as previously described.[2,3] Thiazole orange (TO_{B6}) **(3)** synthesis is described in **SA.1.1**. and thiazole orange (TO_{Q6}) **(4)** carboxylic acid was synthesised according to a previously determined protocol.[4–6]

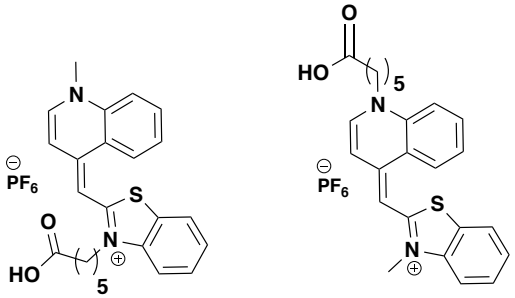

(3) TO_{B6} (4) TO_{Q6}

SA.1.1. Synthesis of TO_{B6} (3):

SA.1.1 a) Synthesis of Reagents (1) and (2)

Synthesis of 3-(5-carboxypentyl)-2-methylbenzo[*d*]thiazolium bromide **(1)** was carried out as previously described and all spectroscopic data agrees with the literature.[7] Synthesis of 4-chloro-1-methylquinolin-1-ium trifluoromethanesulfonate **(2)** was carried out as previously described and all spectroscopic data agrees with the literature.[8]

SA.1.1 b) Synthesis of 3-(5-carboxypentyl)-2-((1'-methylquinolin-4'(1H)-ylidene)methyl) benzo [*d*] thiazol-3-ium hexafluorophosphate (TO_{B6}) (3)

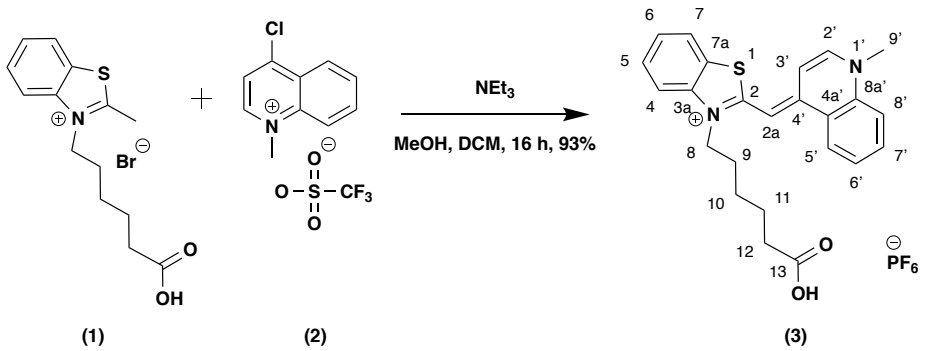

(1) (2) (3)

To a stirred solution of **(1)** (0.93 g, 2.7 mmol, 1.0 eq) and **(2)** (1.05 g, 3.2 mmol, 1.2 eq) in a mixture of dry MeOH (34 mL) and dry CH_2Cl_2 (34 mL) under an argon atmosphere at RT, anhydrous Et_3N (0.94 mL, 6.75 mmol, 2.5 eq) was added. The solution was stirred for 16 h, precipitated with Et_2O (400 mL), filtered and washed with Et_2O (2 x 20 mL). The solution was concentrated and re-dissolved in dry THF (26 mL) and H_2O (24 mL). LiOH (207 mg, 8.4 mmol, 2.5 eq) was added and the solution was stirred for 8 h. To the stirring suspension, HCl (37%, 1.1 mL in 15 mL H_2O) was added, the aqueous layer was extracted with CH_2Cl_2:2-propanol (*v*:*v* = 3:1, 5 x 80 mL). The organic layer was dried with $MgSO_4$, filtered and evaporated to give the product as a red solid. Salt metathesis was performed; $NaPF_6$ (0.8 g, 2.1 eq) was added to a stirred solution of the crude product (0.97 g, 2.2 mmol, 1.0 eq) in CH_2Cl_2:2-propanol (*v*:*v* = 1:3.4, 800 mL). A red solid precipitated and was filtered off, washed with CH_2Cl_2:2-propanol (2 x 10 mL) and H_2O (2 x 15 mL) to give the product as a red solid (0.59 g, 1.07 mmol, 93%).

LRMS (ESI$^+$) m/z (%): 405 $[M\text{-}PF_6]^+$ (100), (Calculated Mass = 405.54)
R_f: 0.37 ($MeOH:CH_2Cl_2$; 15:85)
^{1}H NMR (400 MHz, d_6-DMSO): δ 8.74 (dd, *J* = 8.7, 1.2 Hz, 1H, **$H^{8'}$**), 8.62 (d, *J* = 7.2 Hz, 1H, **$H^{2'}$**), 8.11 – 7.95 (m, 3H; **$H^{6'}$**, **$H^{5'}$** and **H^4**), 7.85 – 7.73 (m, 2H, **$H^{7'}$** and **H^7**), 7.70 – 7.57 (m, 1H, **H^6**), 7.43 (dd, *J* = 8.6, 7.2, 2H, **H^5** and **$H^{3'}$**), 6.94 (s, 1H, **H^{2a}**), 4.63 (t, *J* = 7.4 Hz, 2H, **H^8**), 4.19 (s, 3H, **$H^{9'}$**), 2.21 (t, *J* = 7.2 Hz, 2H, **H^{12}**), 1.82 (m, 2H, **H^9**), 1.61 (m, 2H, **H^{11}**), 1.49 (m, 2H, **H^{10}**).
^{13}C NMR (101 MHz, d_6-DMSO): δ 174.8 (**C^{13}**), 159.1 (**C^2**), 148.6 (**$C^{4'}$**), 145.0 (**$C^{2'}$**), 139.9 (**C^{3a}**), 138.0 (**$C^{8a'}$**), 133.2 (**$C^{6'}$ or $C^{5'}$ or C^4**), 128.2 (**C^6**), 127.1 (**$C^{7'}$**), 125.3 (**$C^{8'}$**), 124.5 (**C^5**), 124.0 (**$C^{4a'}$ or C^{7a}**), 123.8 (**$C^{4a'}$ or C^{7a}**), 122.9 (**$C^{6'}$ or $C^{5'}$ or C^4**), 118.2 (**$C^{6'}$ or $C^{5'}$ or C^4**), 112.9 (**C^7**), 107.9 (**$C^{3'}$**), 87.4 (**C^{2a}**), 45.6 (**C^8**), 42.4 (**$C^{9'}$**), 34.55 (**C^{12}**), 26.7 (**C^9**), 25.8 (**C^{11}**), 24.6 (**C^{10}**).

All spectroscopic data agrees with the literature.[9]

SA.1.2. Oligonucleotide Synthesis:

Solid supports, standard DNA phosphoramidites and all other reagents used in the synthesis were purchased from Link Technologies and Applied Biosystems Ltd. 5-Methyl deoxycytidine phosphoramidite (^{Me}C) was purchased from Link Technologies and 5-(1-propynyl)-deoxycytidine (pC) and amino C6 dT phosphoramidites were purchased from Glen Research (**Figure 1A** in paper).

All oligonucleotides (ODNs) were synthesised using an Applied Biosystems 394 automated DNA/RNA synthesiser using the standard 1.0 µmol phosphoramidite cycle. Stepwise coupling efficiencies were monitored using the automated trityl cation conductivity monitoring facility and for all ODNs were >98.0%. Standard A, G, C and T monomers were coupled for 35 s and non-standard monomers were coupled for 6 min. Standard ODNs were deprotected and cleaved from the solid support using concentrated ammonia solution (1 h, RT) followed by heating in sealed tubes (5 h at 55 °C). TFOs that contained pC phosphoramidite monomers were deprotected for 12 h at 55 °C.

SA.1.3. Oligonucleotide Purification:

ODNs were purified using reverse-phase HPLC on a Gilson system using a Luna 10 µm C8 100 Å 250 x 10 mm column. For unmodified ODNs, the gradient was 3.5% - 50% buffer B over 20 min, flow rate of 4 mL/min (buffer A: 0.1 M triethylammonium bicarbonate (TEAB), buffer B: 0.1 M TEAB with 50% acetonitrile). ODNs with multiple additions of pdU and those that were labelled with TO_{B6} **(3)** or TO_{Q6} **(4)** were purified with hexylammonium acetate (HAA) with a gradient of 60% - 80% buffer B over 30 min, flow rate of 4 mL/min (buffer A: 0.1 M HAA, buffer B: 0.1 M HAA with 50% acetonitrile) and fractions were desalted using two NAP-10 gel filtration columns purchased from GE Healthcare according to the manufacturer's instructions. Elution of ODNs was monitored by ultraviolet absorption at a suitable wavelength in the range 260 – 300 nm. All oligonucleotides were characterised by negative-mode HPLC-mass spectrometry using a Waters Xevo G2-XS QT of mass spectrometer with an Acquity UPLC system, equipped with an Acquity UPLC oligonucleotide BEH C18 column (particle size: 1.7 µm; pore size: 130 Å; column dimensions: 2.1 x 50 mm). Data were analysed using Waters Mass Lynx software. Data is given in **Table S1**.

SA.2. Thiazole Orange Active Ester Labelling Procedure

To form the active ester, TO carboxylic acid **(3 or 4)** (1.1 mg, 2 µmol, 20 eq) was dissolved in 25 µL of DMF with PyBOP (benzotriazol-1-yl-oxytripyrrolidinophosphonium hexafluorophosphate) (1.04 mg, 2 µmol, 20 eq) and 4-methylmorpholine (6 µmol, 60 eq). This solution was shaken at 25 ˚C for 10 min. Once completely dissolved, this solution was added to the ODN (100 nmol, 1 eq) dissolved in 25 µL of $NaHCO_3$ labelling buffer (0.5 M, pH 8.6). The final solution was shaken for 4 h at 37 ˚C. The solution was desalted to remove excess dye using NAP-10 gel filtration columns and purified to produce an average yield of

71.7% for one addition of TO to the TFO. **Note:** This method was used for single-labelled TFOs. For double/triple labelling, TO **(3 or 4)** (30 eq), PyBOP (30 eq) and 4-methylmorpholine (90 eq) were used following the same procedure to produce an average yield of 61.6% for double addition and 38.4% of triple addition of TO (All yields are given in **Table S2**).

SA.3. Click Chemistry Labelling Procedure

A solution of click catalyst was prepared from tris(3-hydroxypropyltriazolylmethyl) amine ligand (THPTA, 10.5 µmol, 70 eq in H_2O) and $CuSO_4 \cdot 5H_2O$ (1.5 µmol, 10 eq in H_2O). The solution was mixed with the ATTO 647N azide (0.5 µmol, 3.3 eq) in 100 µL of DMSO. The mixture was added to the ODN (150 nmol, 1 eq) dissolved in 10 µL of H_2O and sodium ascorbate (15 µmol, 100 eq in H_2O) was added last to begin the reaction. The final solution was shaken for 3 h at 30 ˚C (850 rpm). The solution was desalted to remove excess dye using a NAP-10 followed by a NAP-25 gel filtration column and purified using HPLC to produce 85% yield of labelled ODN.

SA.4. Biophysical (melting) Analysis Buffers

pH 5.8	High Mg^{2+} Buffer:	10 mM Na phosphate, 10 mM $MgCl_2$
	Low Mg^{2+} Buffer:	10 mM Na phosphate, 150 mM NaCl, 2 mM $MgCl_2$
pH 7	High Mg^{2+} Buffer:	10 mM MOPS, 10 mM $MgCl_2$
	Low Mg^{2+} Buffer:	10 mM MOPS, 150 mM NaCl, 2 mM $MgCl_2$
pH 8	High Mg^{2+} Buffer:	10 mM HEPES, 10 mM $MgCl_2$
	Low Mg^{2+} Buffer:	10 mM HEPES, 150 mM NaCl, 2 mM $MgCl_2$

SA.5. UV Thermal Denaturation Studies

Thermal denaturation studies were carried out on a Cary 4000 UV-Visible Spectrophotometer from Varian in Hellma® SUPRASIL synthetic quartz cuvettes of 10 mm path-length and 1 mL sample volume. The measurements were monitored at 260 nm using Cary WinUV thermal application software. The TFO and duplex were combined in a concentration/ratio of 2.5:1 µM for all triplexes and dissolved in the appropriate filtered buffer (analysis was carried out in all 6 buffers, see **SA.4** for buffer composition). The first ramp equilibrated the samples by initial denaturation by heating to 85 ˚C at 10 ˚C/min. The samples were held at this temperature for 2 min before annealing was carried out by cooling to 20 ˚C at a rate of 0.5 ˚C/min and holding for 20 min. Heating was at a rate of 0.5 ˚C/min and samples were held at 85 ˚C for 2 min. A total of six ramps are carried out but the first (fast) ramp was excluded to ensure uniform results and an average T_m was determined from the first derivatives of the melting curves. Final T_m values are an average of two individual measurements in which each is an average of 5 ramps and produced errors within ±0.6 ˚C.

SA.6. Fluorescence Melting Studies

Fluorescence melting experiments were conducted on a CFX96™ Real-Time PCR Detection System (Bio-Rad Laboratories Inc.) using Bio-Rad CFX Manager 3.0 software. Samples of 0.25 µM of the duplex in 20 µL filtered buffer were used with TFO concentration of 0.625 µM to provide a ratio of [2.5:1] (analysis was carried out in all 6 buffers, see **SA.4** for buffer composition). The samples were pre-incubated at 25 ˚C for 1 min. They were denatured by heating to 95 ˚C at a rate of 0.1 ˚C/s then held at 95 ˚C for 5 min before cooling to 25 ˚C at the same rate. They were held at 25 ˚C for 5 min then denatured by heating to 95 ˚C at a rate of 0.6 ˚C/min before holding at 95 ˚C for 5 min. The samples were then cooled to 25 ˚C at the same rate. The fluorescence melting curve data was converted to the first derivatives to give the melting temperatures (-d(F)/dT where F is the fluorescence and T is temperature in ˚C). Steps 3 (slow melting steps) and steps 4 (slow annealing steps) were used for data analysis. The excitation and emission channel used on the CFX96™ Real-Time PCR Detection System for TO was the TET™ dye channel (λ_{ex} = 521 nm, λ_{em} = 536 nm) and for ATTO 647N was Cy5 dye channel (λ_{ex} = 650 nm, λ_{em} = 670 nm).

SA.7. Steady State Fluorescence Measurements

Fluorescence studies were performed on a Perkin Elmer LS50B Luminescence Spectrometer fitted with Perkin Elmer PTP-1 Peltier temperature controller. *FLWinlabTempScan* software was used with 400 nm/s scan speed. The emission was recorded from 510 nm to 700 nm, excitation wavelength = 484 nm, gain = high (900V), excitation slit width = 7 nm and emission slit width = 7 nm. Final concentrations of the samples were 1.8 µM of the duplex in 250 µL buffer and 1 µM of TFO (analysis was carried out in High Mg^{2+} buffers at pH 5.8 and pH 7, see **SA.4** for buffer composition). Duplex samples were pre-annealed at 95 ˚C for 5 min before being allowed to cool to RT overnight. On addition of the duplex to the TFO sample, samples were left for 400 s to allow complete formation of the triplex (SPR analysis provided the formation time of the triplex). Spectra were recorded for the single stranded TFO and then titrated with 1.8 eq of the target duplex and recorded again at 20 ˚C. Fluorescence intensity ratios were calculated by comparison of the fluorescence intensity at the maximum emission wavelength of the ssTFO (λ_{em}^{ss}) and the formed triplex(λ_{em}^{T}). Final fluorescence values were calculated from an average of two individual measurements in which both the ssTFO and formed triplex were measured and produced errors within ±5.4%.

SA.8. Quantum Yield Analysis

The absolute fluorescence quantum yields were measured using a SC-30 integrating sphere module (Edinburgh Instruments) and the re-absorption effect was corrected when possible. For all TFOs and formed triplex complexes, the excitation wavelength was 488 nm, the wavelength step size 0.1 nm and integration dwell time 0.2 s. All fluorescence samples were prepared with optical densities under 0.1 under ambient conditions (1 µM of TFO in 3000 µL of buffer, analysis was carried out in High Mg^{2+} buffers at pH 5.8 and pH 7, see **SA.4** for

buffer composition). Sample spectra were recorded for the single stranded TFO and then titrated with 1.8 eq of the target duplex, allowed anneal for 400 s and recorded again at 20 ˚C. Three scans were repeated for both the TFO and triplex sample solutions as well as the buffer. The scattering region between 483 nm and 593 nm, and emission region between 500 and 700 nm were chosen for the calculation of the observed quantum yields.

SA.9. Gel Electrophoresis

Triplex formation was analysed by constant voltage native polyacrylamide gel electrophoresis. 15% polyacrylamide gels (40% acrylamide; acrylamide:bisacrylamide 29:1) were run at RT at 5 V/cm (125 V) for 18 h using 40 mM MOPS buffer containing 10 mM NaOAc and 10 mM $MgCl_2$ (pH 7). Samples were annealed at 90 ˚C for 5 min and slowly cooled to RT overnight before loading. The concentration of each duplex strands was 1 µM in 25 µL (25 pmol) with varying ratios of TFO strand as indicated in the **Figure 4** in the paper. Samples were loaded in 10% glycerol and the same MOPS running buffer. After electrophoresis, gels were visualised using fluorescence light for samples labelled with TO_{B6} **(3)**. For unlabelled samples, gels were stained with SYBR Gold and imaged.

SA.10. Surface Plasmon Resonance

SPR measurements were carried out on a BIACore X100 instrument (GE Healthcare). Biosensor chips, pre-coated with streptavidin (GE Healthcare), were used throughout the experiment and the running buffer was 10 mM MOPS, 10 mM $MgCl_2$ (pH 5.8). The sensor chip surface was pre-treated prior to immobilisation with 3 serial injections of 1M NaCl in 50 mM NaOH followed by a prime with running buffer at 25 ˚C. A 3'-biotinylated Py strand of the duplex was passed over the surface at 10 µL/min until the target immobilisation response (Imm RU) was achieved, corresponding to 700 response units (RU).

A solution of Pu strand of the duplex (10 µM for 240 s contact time) was passed over the chip surface at 5 µL/min to form a duplex on the surface and allowing a 360 s stabilisation period. Solutions containing 0.4, 0.5, 0.6, 0.7, 0.8, 0.9, 1.0, 2.5, 5, 10 or 20 µM of the TFO (for 420 s contact time) were then injected over the immobilized duplex at a flow rate of 5 µL/min to generate the triplex. 1800 s were allowed for dissociation of the triplex. The surface was regenerated using NaOH at a flow rate of 10 µL/min (10 mM for 240 s contact time) and re-equilibrated with running buffer (360 s) before the next cycle was begun. Association and dissociation rate constants were determined for the triplexes using the BIACore X100 Evaluation Software 2.0.1 Plus Package which fits experimental data to ideal curves by non-linear curve fitting methods. The model used assumes 1:1 binding and that the kinetics are first-order, and not limited by mass transport effects.[10]

Section B. Supplementary Data

Table S1: Mass Spectrometry Data for All Oligonucleotides

ODN	Modification	Sequence	Cal. Mass	Found Mass
TRIP-T	Unlabelled	5′ – TTT TTM TTT MTM TMT	4497	4497.1
	1x pdU	5′ – TTT TTM TTP MTM TMT	4536	4538.0
	1x TO	5′ – TTT TTM TTT MTM TMT	4923	4923.7
	2x pdU	5′ – TTP TTM TTP MTM TMT	4575	4576.1
	2x TO	5′ – TTT TTM TTT MTM TMT	5349	5349.0
	3x pdU	5′ – TTP TTM TTP MTM PMT	4614	4615.2
	3x TO	5′ – TTT TTM TTT MTM TMT	5772	5773.2
	Pu Target	5′ – GGA AGG GGG AAA AAG AAA GAG AGA GGA GAG AGG	10546	10547.0
	Py Target	3′ – CCT TCC CCC TTT TTC CTC CTC TCT CCT CTC TCC	9721	9722.2
TRIP-T_i	Control	5′ – TTT TTM TTT MTM TMT	4193	4192.1
	Unlabelled	5′ – TTT TTM T^{P}CT MTM TMT	4698	4699.3
	1x pdU	5′ – TTT TTM T^{P}CP MTM TMT	4559	4561.1
	1x TO	5′ – TTT TTM T^{P}CT MTM TMT	4946	4947.0
	2x pdU	5′ – TTP TTM T^{P}CP MTM TMT	4598	4600.2
	2x TO	5′ – TTT TTM T^{P}CT MTM TMT	5372	5372.0
	3x pdU	5′ – TTP TTM T^{P}CP MTM PMT	4637	4638.4
	3x TO	5′ – TTT TTM T^{P}CT MTM TMT	5798	5799.5
	Pu Target	5′ – GGA AGG GGG AAA AAG ACA GAG AGA GGA GAG AGG	10522	10522.1
	Py Target	3′ – CCT TCC CCC TTT TTC CGC CTC TCT CCT CTC TCC	9746	9746.4
TRIP-C	Unlabelled	5′ – CTM CCM MCC MCC TMT MTC	5287	5288.2
	1x pdU	5′ – CTM CCM MCC MCC PMT MTC	5326	5327.0
	1x TO	5′ – CTM CCM MCC MCC TMT MTC	5711	5712.4
	2x pdU	5′ – CPM CCM MCC MCC PMT MTC	5366	5363.5
	2x TO	5′ – CTM CCM MCC MCC TMT MTC	6138	6137.0
	3x pdU	5′ – CPM CCM MCC MCC PMT MPC	5405	5405.0
	3x TO	5′ – CTM CCM MCC MCC TMT MTC	6564	6562.6
	Pu Target	5′ – GGA AAA AAG GAG GGG GGG GGG AGA GAG AAG AGA AGG	11549	11550.0
	Py Target	3′ – CCT TTT TTC CTC CCC CCC CCC TCT CTC TTC TCT TCC	10574	10574.1

ODN	Modification	Sequence	Cal. Mass	Found Mass
TRIP-C$_i$	Control	**5′ – CTM CCT MCC MCC TMT MTC**	5530	5530.5
	Unlabelled	**5′ – CTM CC^{P}C MCC MCC TMT MTC**	5328	5328.4
	1x pdU	**5′ – CTM CC^{P}C MCC MCC PMT MTC**	5351	5352.0
	1x TO	**5′ – CTM CC^{P}C MCC MCC TMT MTC**	5738	5739.0
	2x pdU	**5′ – CPM CC^{P}C MCC MCC PMT MTC**	5390	5391.0
	2x TO	**5′ – CTM CC^{P}C MCC MCC TMT MTC**	6164	6165.0
	3x pdU	**5′ – CPM CC^{P}C MCC MCC PMT MPC**	5429	5429.9
	3x TO	**5′ – CTM CC^{P}C MCC MCC TMT MTC**	6590	6591.4
	Pu Target	**5′ – GGA AAA AAG GAG GGC GGG GGG AGA GAG AAG AGA AGG**	11484	11485.3
	Py Target	**3′ – CCT TTT TTC CTC CCG CCC CCC TCT CTC TTC TCT TCC**	10638	10637.5
TRIP-TC	3x pdU	**5′ – MPM TMT TMP MTT MPM**	4611	4611.0
	3x TO	**5′ – MTM TMT TMT MTT MTM**	5770	5770.3
	Pu	**5′ – GGA AGG GAA GAG AGA AGA GAA GAG GGA GAG AGG**	10562	10563.5
	Py	**3′ – CCT TCC CTT CTC TCT TCT CTT CTC CCT CTC TCC**	9706	9707.5
TRIP-C$_i$ Varied Linker	1x AE	**5′ – CTM CCM MCC MCC L$_2$MT MTC**	5347	5345.6
	1x TO	**5′ – CTM CCM MCC MCC T$_{L2}$MT MTC**	5734	5732.6
	1x AC6	**5′ – CTM CCM MCC MCC L$_3$MT MTC**	5442	5442.6
	1x TO	**5′ – CTM CCM MCC MCC T$_{L3}$MT MTC**	5829	5828.4
Mismatch Duplexes	Pu-T	**5′ – GGA AGG GGG AAA AAG ATA GAG AGA GGA GAG AGG**	10537	10538.5
	Py-A	**3′ – CCT TCC CCC TTT TTC CAC CTC TCT CCT CTC TCC**	9730	9731.7
	Pu-G	**5′ – GGA AGG GGG AAA AAG AGA GAG AGA GGA GAG AGG**	10562	10563.0
	Py-C	**3′ – CCT TCC CCC TTT TTC CCC CTC TCT CCT CTC TCC**	9706	9707.8
ATTO-TOTFO TRIP-T$_i$	5′-alkyne 1x pdU	**5′ – alk-TTT TTM T^{P}CP MTM TMT**	4719	4720.0
	5′-ATTO 1x TO	**5′ – ATTO-TTT TTM T^{P}CT MTM TMT**	5952	5950.6
	3′-alkyne 1x pdU	**5′ – TTT TTM T^{P}CP MTM TMT-alk**	4894	4894.0
	3′-ATTO 1x TO	**5′ – TTT TTM T^{P}CT MTM TMT-ATTO**	6126	6127.0
TRIP-T$_i$	Biotinylated Py	**3′ – CCT TCC CCC TTT TTC CGC CTC TCT CCT CTC TCC-bio**	10315	10317.1

ODN	Modification	Sequence	Cal. Mass	Found Mass
Scrambled Duplex	Pu	**5′ – GGA AGG GGG AGA AGA AGA AGA GAA GGA GAA AGG**	10546	10547.0
	Py	**3′ – CCT TCC CCC TCT TCT TCT TCT CTT CCT CTT TCC**	9721	9722.0

Pu = polypurine duplex strand, **Py** = polypyrimidine duplex strand, **P** = propargylamino-deoxyuridine (pdU), **T** = Thiazole orange attached through propargylamino linker, $\mathbf{L_2}$ = 2′-amino-ethoxy-deoxythymidine (AE), $\mathbf{T_{L2}}$ = Thiazole orange attached through 2′-aminoethoxy linker, $\mathbf{L_3}$ = Amino-C6-deoxythymidine (AC6), $\mathbf{T_{L3}}$ = Thiazole orange attached through amino-C6 linker, **M** = 5-methyl deoxycytidine, **^{P}C** = 5-(1-propynyl)-2′-deoxycytidine (pC), **alk =** alkyne attachment, **ATTO =** ATTO 647N, **bio** = Biotin TEG.

Table S2: Yields and Mass Spectrometric Analysis of TO-labelled TFOs

A

ODN	Modification	Sequence	Yield
TRIP-T	1x TO	5′ – TTT TTM TTT MTM TMT	70.8%
	2x TO	5′ – TTT TTM TTT MTM TMT	56.7%
	3x TO	5′ – TTT TTM TTT MTM TMT	35.8%
TRIP-T_i	1x TO	5′ – TTT TTM T^{P}CT MTM TMT	82.5%
	2x TO	5′ – TTT TTM T^{P}CT MTM TMT	65.2%
	3x TO	5′ – TTT TTM T^{P}CT MTM TMT	33.8%
TRIP-C	1x TO	5′ – CTM CCM MCC MCC TMT MTC	62.0%
	2x TO	5′ – CTM CCM MCC MCC TMT MTC	59.7%
	3x TO	5′ – CTM CCM MCC MCC TMT MTC	42.1%
TRIP-C_i	1x TO	5′ – CTM CC^{P}C MCC MCC TMT MTC	71.3%
	2x TO	5′ – CTM CC^{P}C MCC MCC TMT MTC	64.6%
	3x TO	5′ – CTM CC^{P}C MCC MCC TMT MTC	49.1%
TRIP-TC	3x TO	5′ – MTM TMT TMT MTT MTM	31.3%

B

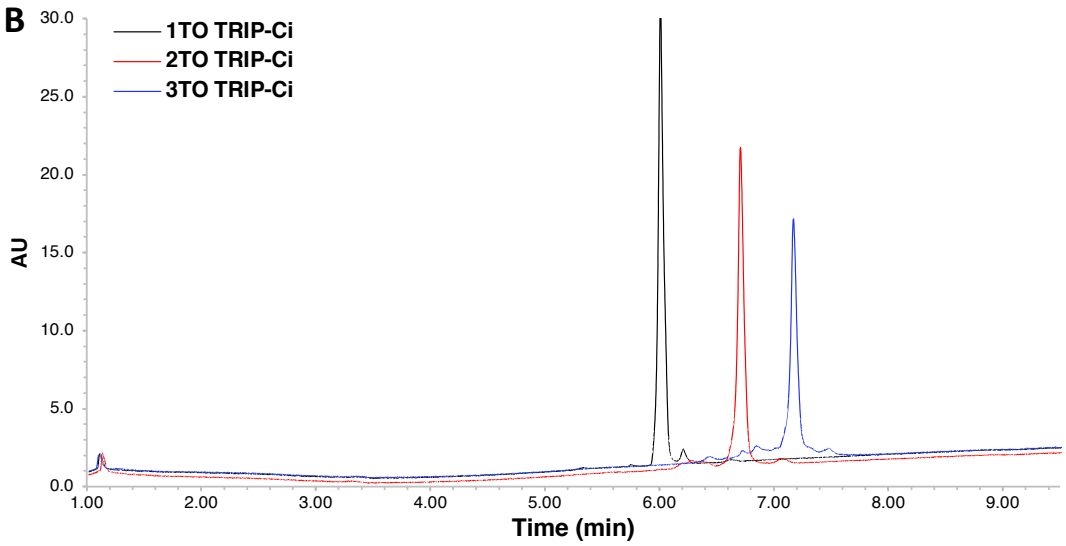

A) Experimental yields of TFOs labelled with single/multiple TO through active ester labelling (See **SA.2** for experimental details). **T** = Thiazole orange attached through propargylamino linker, **M** = 5-methyl deoxycytidine, **^{P}C** = 5-(1-propynyl)-2′-deoxycytidine (pC).

B) UPLC-MS chromatograms of pure 1xTO, 2xTO and 3xTO labelled TFO-C_i. Labelled TFOs were produced in yields according to (A) and mass was confirmed according to **Table S1**. **UPLC x-axis** = time (min) and **y-axis** = UV absorbance at 260nm.

Figure S1: Optimisation of Linker for Attachment of TO to TFO-C

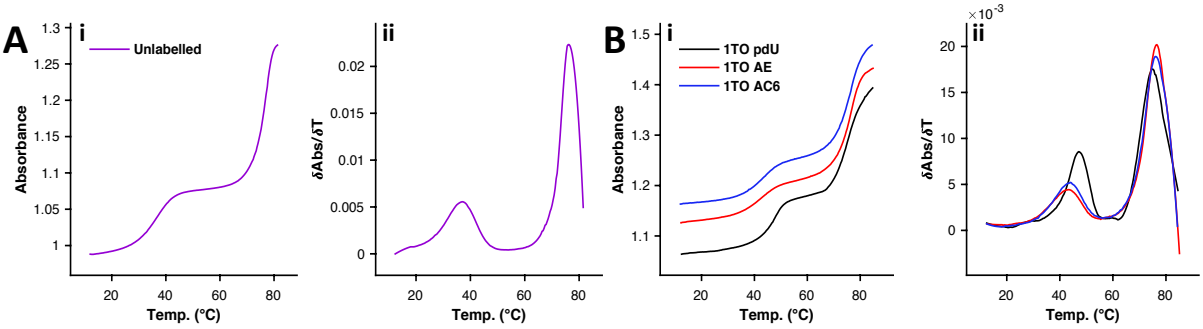

C

Triplex	Sequence	T_m (°C)	ΔT_m
Unlabelled TFO-C	5′ – CTM CCM MCC MCC TMT MTC	35.6	-
1x TO pdU TFO-C	5′ – CTM CCM MCC MCC **T**MT MTC	46.2	+10.6
1x TO AE TFO-C	5′ – CTM CCM MCC MCC $\mathbf{T}_{L2}$MT MTC	44.6	+9.0
1x TO AC6 TFO-C	5′ – CTM CCM MCC MCC $\mathbf{T}_{L3}$MT MTC	45.0	+9.4

5-(1-propargylamino)-dU (pdU), 2'-aminoethoxy T (AE) and amino C6-dT (AC6) were investigated as linkers for the attachment of TO_{B6}. TFO-C sequence was used to investigate linker efficiency in the formation of TRIP-C. pdU provided the best triplex stabilisation with TO and gave a sharper and more intense melting transition for 1xTO pdU (B).

A) **(i)** Plot of UV melting of unlabelled TRIP-C recorded as a function of temperature (25-90 ˚C). **(ii)** Smoothed first derivative of melting curve shown in (i). *Buffer:* 10 mM phosphate, 150 mM NaCl, 2 mM $MgCl_2$ at pH 5.8.

B) **(i)** Plot of UV melting of 1xTO pdU TRIP-C, 1xTO AE TRIP-C and 1xTO AC6 TRIP-C recorded as a function of temperature (25-90 ˚C). **(ii)** Smoothed first derivative of melting curve shown in (i). *Buffer:* 10 mM phosphate, 150 mM NaCl, 2 mM $MgCl_2$ at pH 5.8.

C) T_m data were obtained from the maxima of the first derivatives of the melting curves. Final T_m values are an average of two individual measurements in which each is an average of 5 ramps. **T** = Thiazole orange attached through propargylamino linker, $\mathbf{T}_{L2}$ = Thiazole orange attached through aminoethoxy linker, $\mathbf{T}_{L3}$ = Thiazole orange attached through amino-C6 linker, **M** = ^{Me}C.

Figure S2: UV Thermal Denaturation Curves for TRIP-T TO_{Q6} at pH 5.8

A

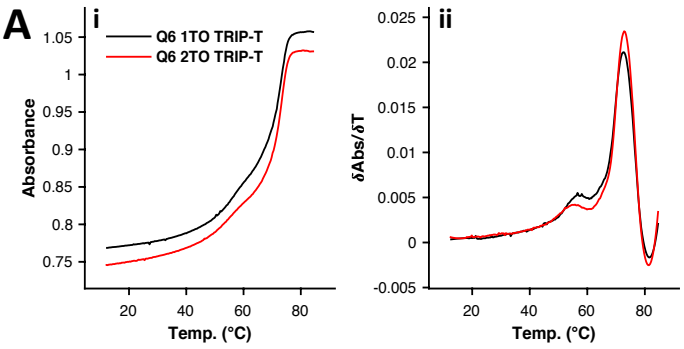

B

Triplex	T_m (°C)
1xTO TRIP-T Q_6	57.4
2xTO TRIP-T Q_6	55.1

A) **(i)** Plot of UV melting of TRIP-T TO_{Q6} recorded as a function of temperature (25–85 ˚C). **(ii)** Smoothed first derivative of thermal denaturation curve shown in (i). The first transition represents triplex denaturation, the second (higher temperature) transition is the duplex denaturation. T_m values are according to the table (B). *Buffer:* 10 mM phosphate, 10 mM $MgCl_2$ at pH 5.8.

B) T_m values were obtained from the maxima of the first derivatives of the melting curves. Final T_m values are an average of two individual measurements in which each is an average of 5 ramps.

Figure S3: Melting Analysis of TRIP-T_i Triplex at pH 7

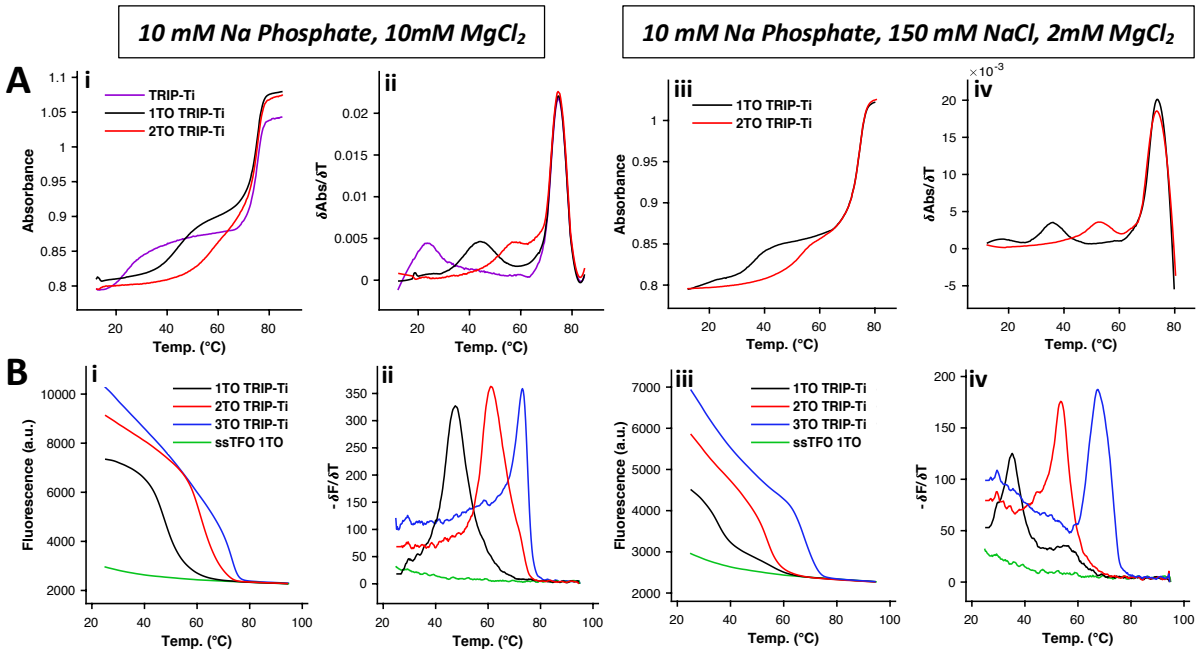

A) **(i)/(iii)** Plot of UV melting of TRIP-T_i recorded as a function of temperature (25–85 ˚C) in the given buffers. **(ii)/(iv)** Smoothed first derivative of thermal denaturation curves. The first transition represents triplex denaturation, the second (higher temperature) transition is the duplex denaturation. T_m values are according to **Table S3.**

B) **(i)/(iii)** Plot of fluorescence melting of TRIP-T_i recorded as a function of temperature (25-90 ˚C) with ssTFO as a control (green) in the given buffers. **(ii)/(iv)** Smoothed first derivative of fluorescence curve shown. T_m values are according to **Table S3**.

Table S3: Melting Temperatures of Triplexes Analysed

Triplex	pH 5.8				pH 7			
	UV		Fluorescence		UV		Fluorescence	
	High Mg^{2+}	Low Mg^{2+}	High Mg^{2+}	Low Mg^{2+}	High Mg^{2+}	Low Mg^{2+}	High Mg^{2+}	Low Mg^{2+}
	T_m (°C)				T_m (°C)			
TRIP-T	43.2	31.9	-	-	39.3	28.4	-	-
1xTO TRIP-T	66.5	58.0	72.2	53.9	60.0	50.6	51.6	42.6
2xTO TRIP-T	n.d.	65.1	76.4	71.7	65.5	58.7	71.9	61.2
3xTO TRIP-T	n.d.	n.d.	78.0	76.7	n.d.	n.d.	74.0	72.0
TRIP-T_i Control	49.0[a]	29.6[a]	-	-	-	-	-	-
TRIP-T_i	50.3	31.2	-	-	23.0	-	-	-
1xTO TRIP-T_i	66.3	48.7	66.0	47.0	45.0	35.9	47.6	32.3
2xTO TRIP-T_i	n.d.	66.9	74.6	65.1	57.5	51.3	61.8	50.0
3xTO TRIP-T_i	n.d.	n.d.	76.1	73.2	n.d.	n.d.	73.4	65.9
TRIP-C	44.0	35.6	-	-	*nt*	*nt*	-	-
1xTO TRIP-C	50.6	46.2	49.1	44.1	25.7	19.9	n.d.	n.d.
2xTO TRIP-C	n.d.	55.1	54.3	52.4	30.4	26.0	n.d.	n.d.
3xTO TRIP-C	n.d.	61.8	62.5	64.0	34.6	34.8	n.d.	n.d.
TRIP-C_i Control	31.5[a]	21.0[a]	-	-	-	-	-	-
TRIP-C_i	39.5	26.6	-	-	*nt*	*nt*	-	-
1xTO TRIP-C_i	42.9	29.7	48.0	30.5	*nt*	*nt*	*nt*	*nt*
2xTO TRIP-C_i	45.3	36.7	n.d.	42.4	*nt*	*nt*	*nt*	*nt*
3xTO TRIP-C_i	56.4	44.7	n.d.	48.1	25.4	24.7	n.d.	n.d.
TRIP-TC	77.0	72.7	-	-	52.6	49.0	-	-
3xTO TRIP-TC	80+	80+	86.7	76.3	75.3	80+	73.2	73.4

T_m data were obtained from the maxima of the first derivatives of the UV or fluorescence melting curves. Final T_m values for UV melting are an average of two individual measurements in which each is an average of 5 ramps. Final T_m values for fluorescence melting are an average of two individual measurements. **n.d. =** not determined. ***nt* =** not triplex formation observed. **[a] =** Control triplex contains a T instead of pC modification.

Figure S4: UV Thermal Denaturation Curves of Scrambled Sequences at pH 7

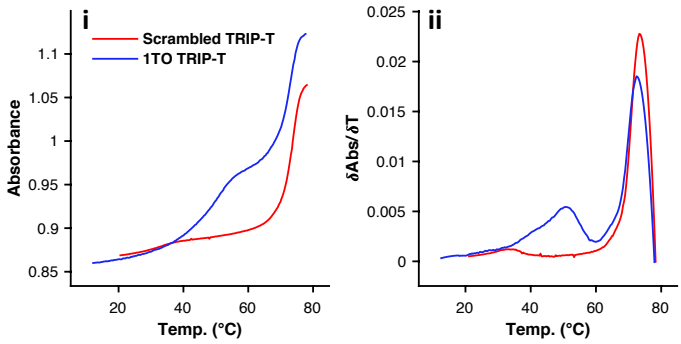

No triplex formation was observed when 1xTO TFO-T was mixed with the scrambled duplex indicating that TO only intercalates in a sequence-specific manner.

(i) Plot of UV absorption of 1xTO scrambled TRIP-T and 1xTO TRIP-T (T_m = 50.6 ˚C) recorded as a function of temperature (25–85 ˚C). **(ii)** Smoothed first derivative of thermal denaturation curve shown in (i). *Buffer:* 10 mM MOPS, 150 mM NaCl, 2 mM $MgCl_2$ at pH 7.

Figure S5: Fluorescence Melting of Triplexes containing mismatched triplets

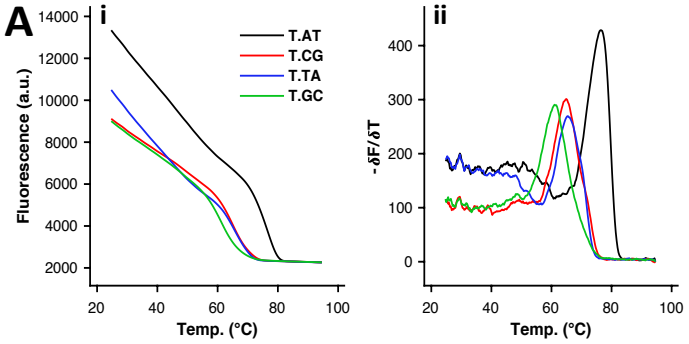

B

Triplex	pH 7
TRIP-T containing:	**T_m (°C)**
3xTO T.AT	72.0
3xTO T.CG	62.2
3xTO T.TA	62.0
3xTO T.GC	58.2

Mismatched triplet studies demonstrate a triplet stability order of T.AT > T.CG (-9.8 ˚C) > T.TA (-10.0 ˚C) > T.GC (-13.8 ˚C). This confirms that TO intercalation in the TFO does not destroy target duplex selectivity.

A) **(i)** Plot of fluorescence melting of 3xTO TRIP-T triplexes (TRIP-T) recorded as a function of temperature (25–90 ˚C). **(ii)** Smoothed first derivative of fluorescence curve shown in (i). T_m values are given in table (B). *Buffer:* 10 mM MOPS, 150 mM NaCl, 2 mM $MgCl_2$ at pH 7.

B) T_ms were obtained from the maxima of the first derivatives of the melting curves. Final T_m values are an average of two individual measurements.

Figure S6: Structures of Base Triplets

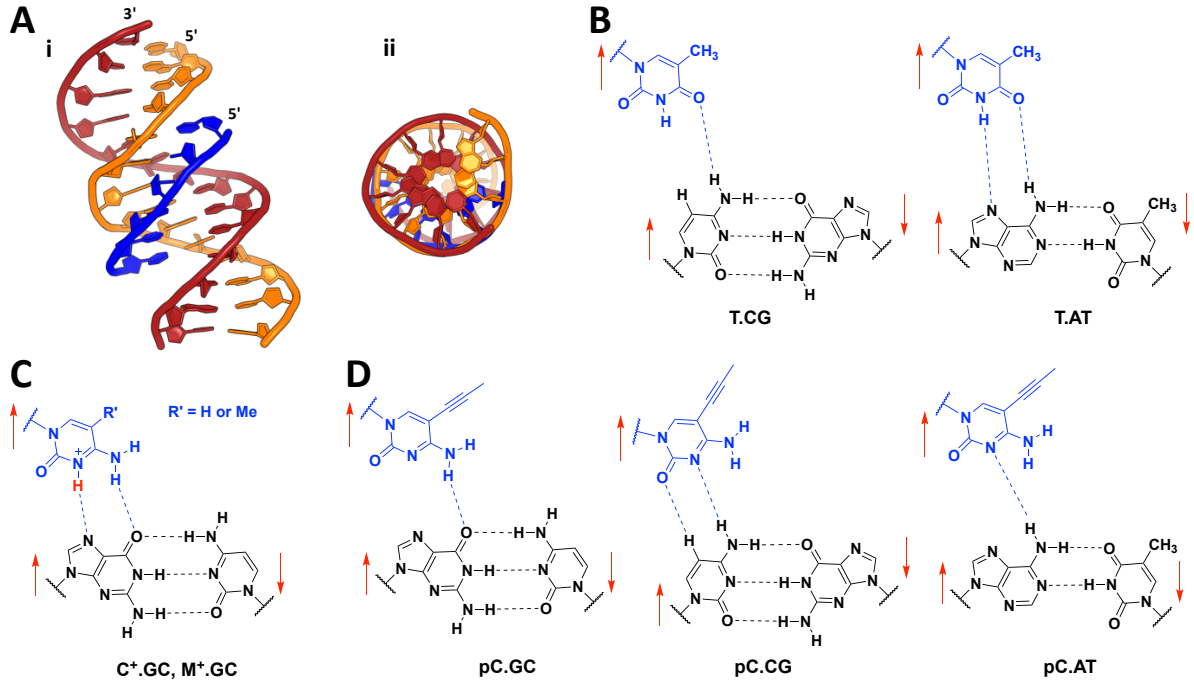

A) **i)** Side view and **ii)** top view of DNA parallel triplex with the TFO (blue) bound in the major groove of the duplex[11].

B) Thymine base in the TFO recognises C or A in the duplex; but with a single H-bond for C-recognition. Red arrows indicate relative directionality of DNA strands.

C) C and ^{Me}C (**M**) in the TFO recognise G in the duplex.

D) Triplets involving pC in the TFO; the low pk_aH of pC compared to C or ^{Me}C leads to destabilisation of the triplet with GC as pH increases. The triplet with AT also is unstable with a single H-bond, whereas in the triplet with CG, two H-bonds between pC and C can form (one is a weak C-H···O hydrogen bond). The position of pC relative to the duplex is displaced compared to the other triplets shown. See **Figure S7**.

Figure S7: Fluorescence Melting Curves of pC-Mismatched Triplexes at pH 5.8 and 7

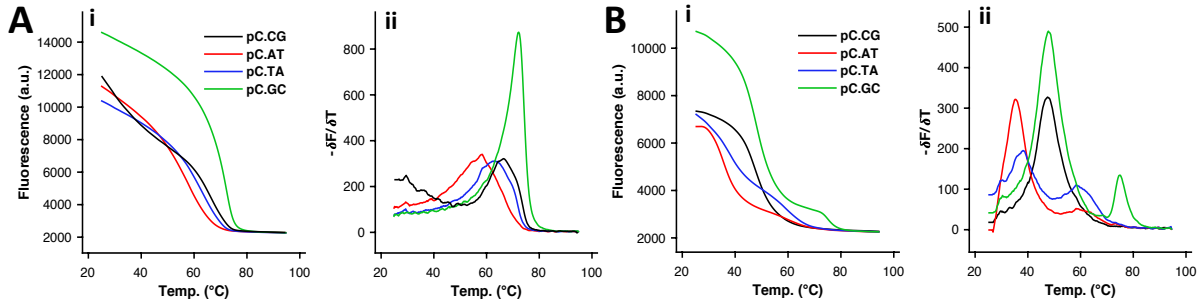

C

Triplex	pH 5.8	pH 7
TRIP-T_i containing:	**T_m (°C)**	
1xTO pC.CG	66.0	47.6
1xTO pC.GC	72.3	47.7
1xTO pC.TA	62.9	37.1
1xTO pC.AT	56.6	35.3
1xTO T.AT (TRIP-T)	66.5	60.0

As described in **Figure S6**, as pH increases the pC.GC triplet becomes less effective (ΔT_m = -24.6 ˚C) while pC.CG is superior (ΔT_m = -18.4 ˚C) highlighting the selectivity of pC.CG for C:G at elevated pH.

A) **(i)** Plot of fluorescence melting of 1xTO mismatch triplexes (TRIP-T_i) recorded as a function of temperature (25-90 ˚C). **(ii)** Smoothed first derivative of fluorescence curve shown in (i). T_m values are according to the table (C). *Buffer:* 10 mM phosphate, 10 mM $MgCl_2$ at pH 5.8.

B) **(i)** Plot of fluorescence melting of 1xTO mismatch triplexes (TRIP-T_i) recorded as a function of temperature (25-90 ˚C). **(ii)** Smoothed first derivative of fluorescence curve shown in (i). T_m values are according to the table (C). *Buffer:* 10 mM MOPS, 10 mM $MgCl_2$ at pH 7.

C) T_m were obtained from the maxima of the first derivatives of the melting curves. Final T_m values are an average of two individual measurements. Comparison of pC.AT with non-inversion triplex T.AT is in red.

Figure S8: Undetermined T_m values from UV Melting Curves of Stable Triplexes

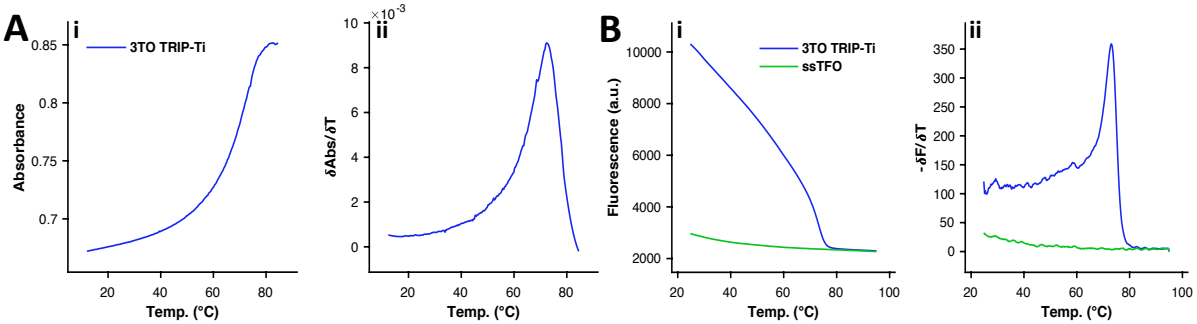

The duplex transition in shown in (A) is broad which can be credited to the triplex transition and duplex transition overlapping. Hence, UV melting is not suitable for determining triplexes T_m values when close to the T_m of the duplex. However, fluorescence melting analysis can be used instead to determine the T_m of the triplex as seen in (B).

A) **(i)** Plot of UV melting of 3xTO TRIP-T_i recorded as a function of temperature (25–85 ˚C). **(ii)** Smoothed first derivative of thermal denaturation curve shown in (i).

B) **(i)** Plot of fluorescence melting of 3xTO TRIP-T_i recorded as a function of temperature (25-90 ˚C). **(ii)** Smoothed first derivative of fluorescence curve shown in (i). *Buffer:* 10 mM MOPS, 10 mM $MgCl_2$ at pH 7.

Table S4: Additional UV Thermal Denaturation Data at pH 8.0

Triplex	UV		Fluorescence	
	10 mM $MgCl_2$	150 mM NaCl 2 mM $MgCl_2$	10 mM $MgCl_2$	150 mM NaCl 2 mM $MgCl_2$
	T_m (°C)			
TRIP-T	30.3	19.5	-	-
3xTO TRIP-T	n.d.	n.d.	51.6	42.6
TRIP-TC	37.0	*nt*	-	-
3xTO TRIP-TC	n.d.	n.d.	53.4	54.4

T_m data were obtained from the maxima of the first derivatives of the corresponding melting curves. Buffers containing 10 mM HEPES at pH 8.0 with varying salt concentrations as according to table. Final T_m values are an average of two individual measurements in which each is an average of 5 ramps. **n.d.** = not determined, ***nt*** = no triplex formation observed.

Figure S9: Fluorescence Intensities of Triplexes

A

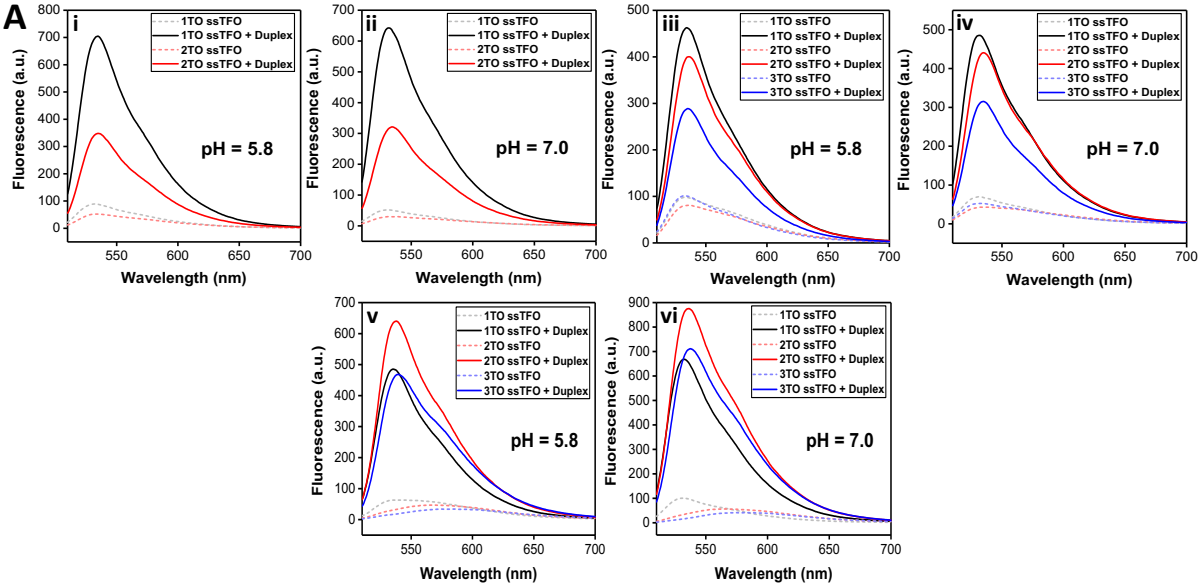

B

Triplex	pH = 5.8			pH = 7.0		
	F^{ss} Area	F^{T} Area	F^{T}/F^{ss}	F^{ss} Area	F^{T} Area	F^{T}/F^{ss}
1xTO TRIP-T	757	15213	20.1	539	11977	22.2
2xTO TRIP-T	5420	37068	6.8	4002	32602	8.1
3xTO TRIP-T	8285	35821	4.3	4917	34086	6.9
1xTO TRIP-T_i	5922	42691	7.2	3467	38824	11.2
2xTO TRIP-T_i	4000	21601	5.4	2517	20097	8.0
1xTO TRIP-C	6011	30493	5.1	6695	41322	6.2
2xTO TRIP-C	4949	41512	8.4	5913	57494	9.7
3xTO TRIP-C	3845	33505	8.7	4438	49113	11.1
1xTO TRIP-C_i	7470	28682	3.8	4803	29731	6.2
2xTO TRIP-C_i	6550	25213	3.8	3950	27565	7.0
3xTO TRIP-C_i	7171	18004	2.5	4118	19425	4.7

A) Fluorescence intensity of 1x, 2x, 3x labelled ssTFO in the absence (dashed line) and presence (solid line) of the duplex. **(i)** TRIP-T_i at pH 5.8 and **(ii)** TRIP-T_i at pH 7 **(iii)** TRIP-C_i at pH 5.8 and **(iv)** TRIP-C_i at pH 7 **(v)** TRIP-C at pH 5.8 and **(vi)** TRIP-C at pH 7. 1.8 µM of duplex and 1 µM of TFO was used. Fluorescence spectra were determined as an average of two individual measurements.

B) Data from fluorescence intensity measurements calculated by integrating the total area under the fluorescence curve from 510 nm to 700 nm. **F^{ss} Area** = fluorescence curve area of the ssTFO, **F^{T} Area** = fluorescence curve area of the triplex, **F^{T}/F^{ss}** = fluorescence intensity ratio calculated by comparison of the ssTFO and the formed triplex area.

In the paper, we analysed the fluorescence intensity at a single wavelength, but by analysing the total area of the fluorescence transition, we observe the same triplex trends although the triplex:single strand intensity ratios are slightly lower.

Table S5: Quantum Yields of Triplexes

Triplex	ϕ^{ss}	ϕ^{T}	ϕ^{T}/ϕ^{ss}
	%	%	
1xTO TRIP-T_i	0.25	5.40	38.6
2xTO TRIP-T_i	0.49	22.80	46.5
3xTO TRIP-T_i	0.44	21.30	48.9
1xTO TRIP-C_i	1.80	19.70	10.9
2xTO TRIP-C_i	0.85	20.20	23.7
3xTO TRIP-C_i	0.56	13.00	23.2

Quantum Yields (QY) were carried out for the triplexes that showed the highest and lowest fluorescence enhancement and range from 5% to 23% depending on the sequence context. Values are an average of two individual measurements. Buffer at pH 7 = 10 mM MOPS, 10 mM $MgCl_2$. **ϕ^{ss} =** quantum yield of single stranded TFO, **ϕ^{T} =** quantum yield of TFO + Duplex, **ϕ^{T}/ϕ^{ss} =** quantum yield upon triplex formation. 1.8 µM of duplex and 1 µM of TFO was used.

Figure S10: Analysis of Dual Dye ATTO-TOTFO

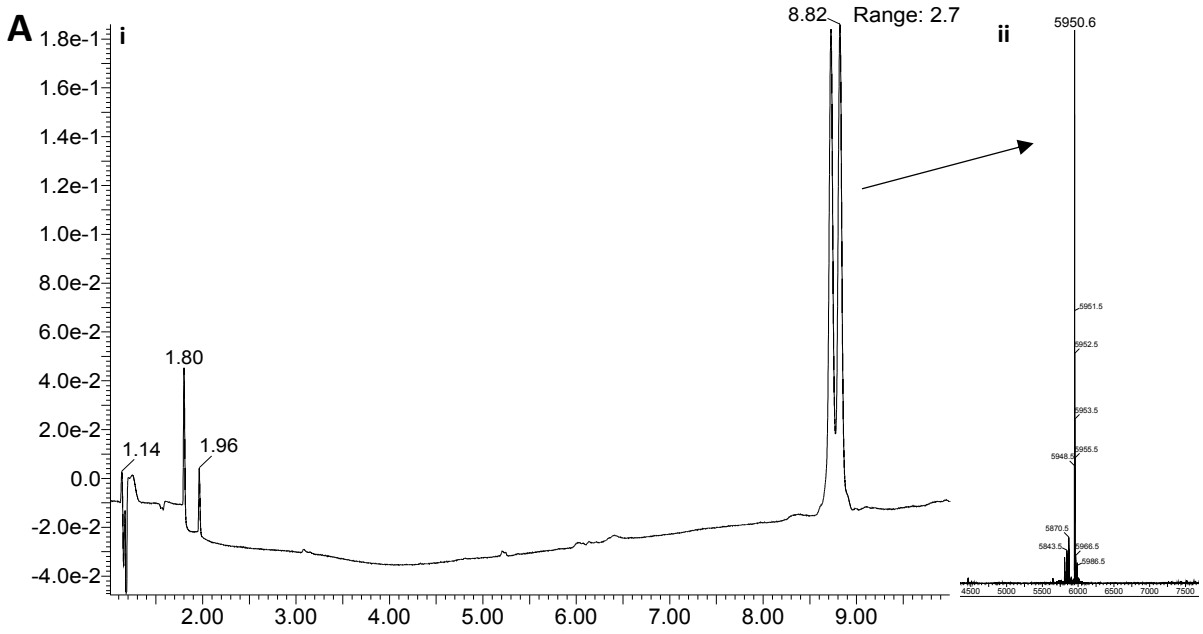

C

Triplex	T_m (°C)
1x TO TRIP-T_i	66.0
5'-ATTO TRIP-T_i	67.7
3'-ATTO TRIP-T_i	66.8

ATTO 647N was conjugated to the 1x TO TFO-T_i using click chemistry at either the 5' or 3' termini (**Section SA.3**). ATTO-TO TFO-T_i was successfully purified by HPLC and characterised by mass spectrometry (**A (i), (ii) and Table S1**). With the addition of ATTO 647N, the stability of the triplex was similar to 1xTO TRIP-T_i. With the second dye attached to the TFO-T_i, fluorescence intensity was greatly increased. Fluorescence intensity is more effective with the dye at the 3' termini of the ATTO-TO TRIP-T_i. Cy5 dye channel (λ_{ex} = 650 nm, λ_{em} = 670 nm) was used to analyse the fluorescence of ATTO 647N.

A) **(i)** UPLC-MS chromatograms of 5'-ATTO TRIP-T_i with mass spectra; *calculated mass = 5952*, found mass = 5950.6. Two peaks are seen on UPLC trace as the dye is a mixture of two regioisomers. **UPLC x-axis =** time (min) and **y-axis =** UV absorbance at 260nm.

B) Plot of fluorescence melting of both 3' and 5' ATTO-TOTFOs recorded as a function of temperature (25-90 ˚C) and smoothed first derivative of fluorescence melting curve. T_m values according to table (C). *Buffer:* 10 mM phosphate, 10 mM $MgCl_2$ at pH 5.8.

C) T_m values were obtained from the maxima of the first derivatives of the melting curves and are an average of two individual measurements.

Figure S11: Mass Spectrometry of Extracted Triplex Band 2xTO TRIP-T_i

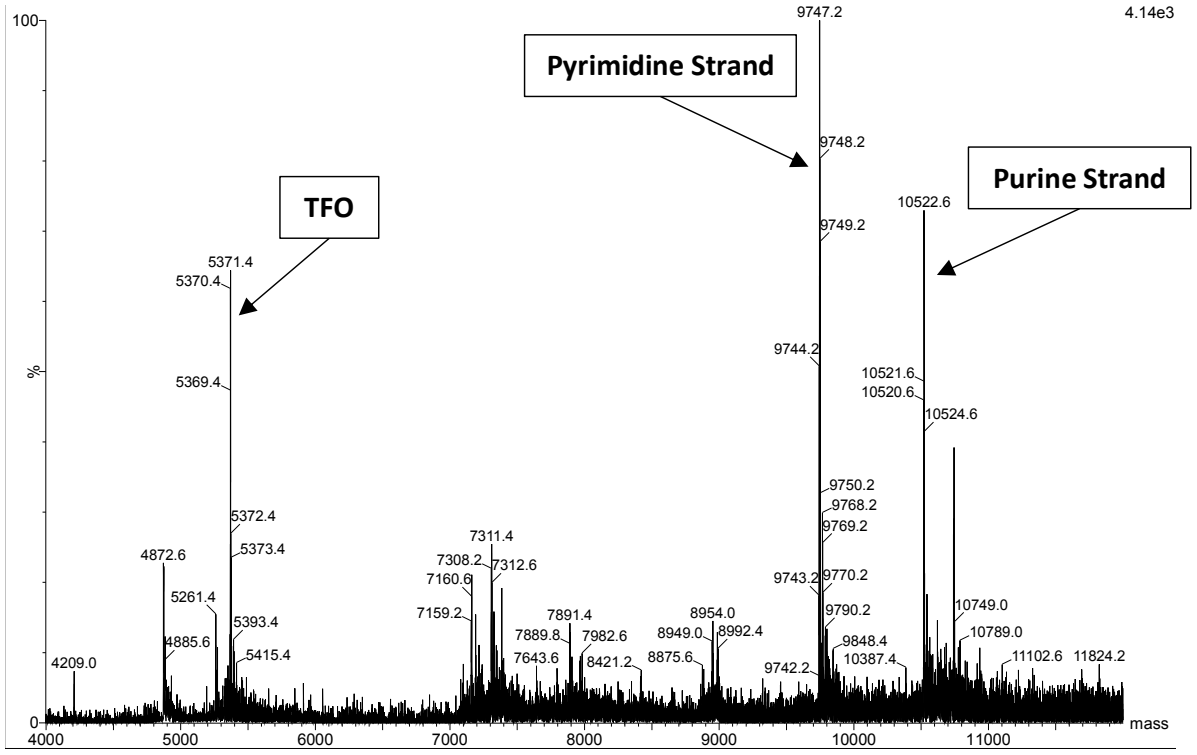

Mass Spectrometry of gel-extracted 2xTO TRIP-T_i triplex (lane 4 of **Figure 4** in paper). Triplex band should contain [1:1] TFO:duplex but can vary due to possible loss of the short TFO during desalting of the gel extract (Gel-filtration). **Purine strand of duplex;** *calculated mass = 10522*, found mass = 10522.6, **Pyrimidine strand of duplex;** *calculated mass = 9746*, found mass = 9747.2 and **2xTO TFO-T_i;** *calculated mass = 5372*, found mass = 5371.4.

Figure S12: SPR Graphs of TRIP-T_i Triplex

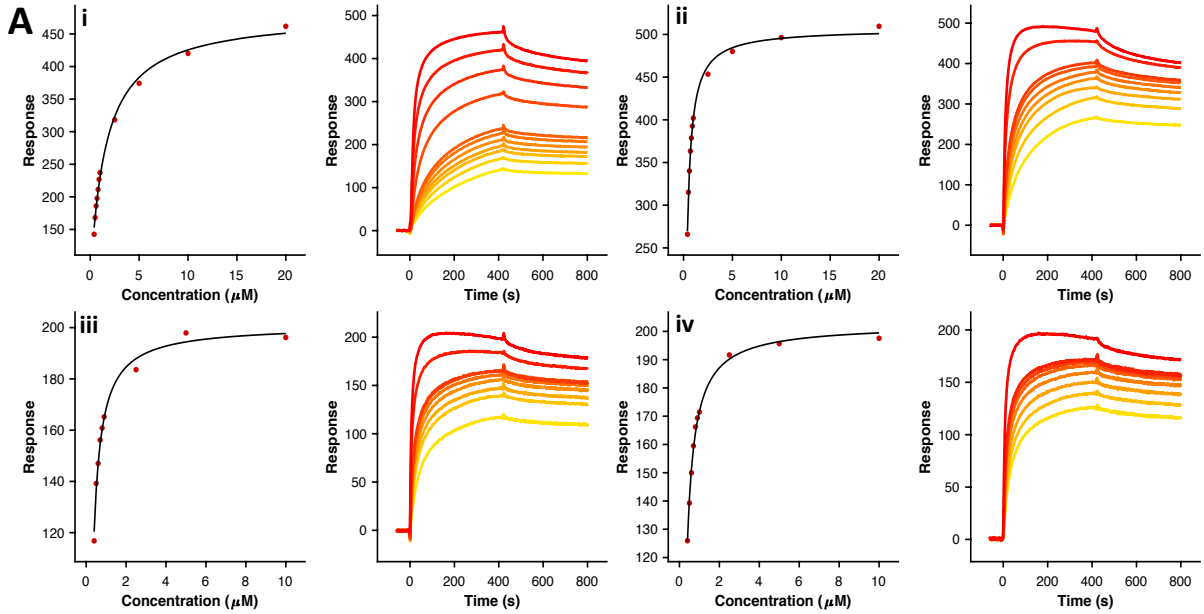

B

Triplex	K_D (M)
TRIP-T_i	1.5 x 10^{-6}
1xTO TRIP-T_i	1.7 x 10^{-8}
2xTO TRIP-T_i	7.7 x 10^{-9}
3xTO TRIP-T_i	3.9 x 10^{-9}

A) SPR analysis of TRIP-T_i triplex formation. **(i)** Binding response of unlabelled triplex, TRIP-T_i plotted against concentration (affinity curve) and binding response plotted against time **(ii)** Binding response of 1xTO TRIP-T_i plotted similarly to (i) **(iii)** Binding response of unlabelled 2xTO TRIP-T_i plotted similarly to (i) **(iv)** Binding response of 3xTO TRIP-T_i plotted similarly to (i). Buffer contains 10 mM MOPS, 10 mM $MgCl_2$, pH 5.8. The concentrations of injected samples ranged from 0.4 µM – 20 µM. See **SA.10** for full experimental details.

B) K_D values were determined using 1:1 steady state binding analysis of both curves.

Section C. References

1 G. R. Fulmer, A. J. M. Miller, N. H. Sherden, H. E. Gottlieb, A. Nudelman, B. M. Stoltz, J. E. Bercaw and K. I. Goldberg, *Organometallics*, 2010, **29**, 2176–2179.

2 K. A. Cruickshank and D. L. Stockwell, *Tetrahedron Lett.*, 1988, **29**, 5221–5224.

3 C. Lou, M. Shelbourne, K. R. Fox and T. Brown, *Chem. - Eur. J.*, 2011, **17**, 14851–14856.

4 T. Sato, Y. Sato and S. Nishizawa, *J. Am. Chem. Soc.*, 2016, **138**, 9397–9400.

5 J. R. Carreon, K. P. Mahon and S. O. Kelley, *Org. Lett.*, 2004, **6**, 517–519.

6 N. Svanvik, G. Westman, D. Wang and M. Kubista, *Anal. Biochem.*, 2000, **281**, 26–35.

7 A. J. Winstead, N. Fleming, K. Hart and D. Toney, *Molecules*, 2008, **13**, 2107–2113.

8 R. Lartia and U. Asseline, *Chem. - A Eur. J.*, 2006, **12**, 2270–2281.

9 S. Ikeda and A. Okamoto, *Chem. - An Asian J.*, 2008, **3**, 958–968.

10 D. J. O'Shannessy, M. Brigham-Burke, K. K. Soneson, P. Hensley and I. Brooks, *Anal. Biochem.*, 1993, 212, 457–468.

11 J. L. Asensio, T. Brown and A. N. Lane, *Structure*, 1999, **7**, 1–11.